

X-ray, optical, and infrared investigation of the candidate supergiant fast X-ray transient IGR J18462–0223

V. Sguera¹, S. P. Drave², L. Sidoli³, N. Masetti¹, R. Landi¹, A. J. Bird², and A. Bazzano⁴

¹ INAF, Istituto di Astrofisica Spaziale e Fisica Cosmica, via Gobetti 101, 40129 Bologna, Italy
e-mail: sguera@iasfbo.inaf.it

² School of Physics and Astronomy, University of Southampton, University Road, Southampton, SO17 1BJ, UK

³ INAF, Istituto di Astrofisica Spaziale e Fisica Cosmica, via E. Bassini 15, 20133 Milano, Italy

⁴ INAF, Istituto di Astrofisica e Planetologia Spaziali, via Fosso del Cavaliere 100, 00133 Rome, Italy

Received 23 November 2012 / Accepted 6 May 2013

ABSTRACT

We report on a broad-band X-ray study (0.5–60 keV) of the poorly known candidate supergiant fast X-ray transient (SFXT) IGR J18462–0223, and on optical and near-infrared (NIR) followup observations of field objects. The out-of-outburst X-ray state has been investigated for the first time with archival INTEGRAL/IBIS, ASCA, *Chandra*, and *Swift*/XRT observations. This allowed us to place stringent 3σ upper limits on the soft (0.5–10 keV) and hard (18–60 keV) X-ray emission of $2.9 \times 10^{-13} \text{ erg cm}^{-2} \text{ s}^{-1}$ and $8 \times 10^{-12} \text{ erg cm}^{-2} \text{ s}^{-1}$, respectively. The source was also detected during an intermediate soft X-ray state with flux equal to $1.6 \times 10^{-11} \text{ erg cm}^{-2} \text{ s}^{-1}$ (0.5–10 keV). In addition, we report on the INTEGRAL/IBIS discovery of three fast hard X-ray flares (18–60 keV) having a duration in the range 1–12 h and the flaring behavior was investigated in soft X-rays (3–10 keV) with archival INTEGRAL/JEM–X observations. The duty cycle (1.2%) and the dynamic ranges (>1380 and >190 in the energy bands 0.5–10 keV and 18–60 keV, respectively) were measured for the first time. Archival UKIDSS *JHK* NIR data, together with our deep *R*-band imaging of the field, unveiled a single, very red object inside the intersection of the *Swift*/XRT and *XMM-Newton* error circles. This source has optical/NIR photometric properties compatible with a very heavily absorbed blue supergiant located at ~ 11 kpc, so is a strong candidate for a counterpart to IGR J18462–0223. NIR spectroscopy is advised to confirm the association. Finally, a hint of a possible orbital period was found at ~ 2.13 days. If confirmed by further studies, this would make IGR J18462–0223 the SFXT with the shortest orbital period among the currently known systems.

Key words. X-rays: binaries – X-rays: individuals: IGR J18462-0223

1. Introduction

The INTEGRAL observatory (Winkler et al. 2003), which was launched in October 2002, has opened a new era in the study of Supergiant high mass X-ray binaries (SGXBs). In fact, the Galactic plane monitoring performed by the INTEGRAL/IBIS instrument (Ubertini et al. 2003) led to the discovery of a new subclass of SGXBs named as supergiant fast X-ray transients (SFXTs). SFXTs host an OB blue supergiant star as the companion donor (Negueruela et al. 2006) and display a peculiar fast X-ray transient behavior that typically lasts a few hours and no longer than a few days at most (Sguera et al. 2005, 2006). The typical dynamic ranges, from X-ray outbursts ($L_X \sim 10^{36} - 10^{37} \text{ erg s}^{-1}$) to the lowest level of X-ray emission, are in the range $10^3 - 10^5$. Such peculiar fast X-ray transient behavior is at odds with the X-ray characteristics of their historical parent population of wind-fed SGXBs, which are detected as bright persistent X-ray sources with typical L_X of $\sim 10^{36} \text{ erg s}^{-1}$.

Although SFXT hunting is not an easy task, in the past few years around ten firm SFXTs have been reported in the literature (see list in Grebenev 2010) along with a similar number of candidate SFXTs (e.g. Sidoli et al. 2012; Fiocchi et al. 2010). The latter are still unidentified X-ray sources that display a fast X-ray transient behavior and an X-ray spectral shape that strongly resembles those from firm SFXTs. However, only infrared/optical follow-up observations of the pinpointed counterpart can provide a firm classification as SFXT, or else its

dismissal (e.g. AX J1749.1–2733, Zurita Heras & Chaty 2008), through the spectroscopical identification of an early-type supergiant star. One of the main aims of the current studies of SFXTs is to collect more detailed spectral/temporal information on poorly known candidate SFXTs, in order to confirm their nature, thereby increasing the sample of established objects. This is mandatory for a population study, to establish e.g. whether SFXTs are a homogeneous class or display a variety of different X-ray characteristics. It is also important to unveil the evolutionary paths and formation rate of SFXTs in our Galaxy, as well as their accretion mechanisms, which are still largely unknown.

Among the candidate SFXTs, IGR J18462–0223 is one of the least studied to date. In the hard X-ray band (20–60 keV), the only information reported in the literature comes from two fast X-ray outbursts detected by INTEGRAL/IBIS (Grebenev & Sunyaev 2010), one in April 2006 (duration and average flux of 1 h and 65 mCrab, respectively) and another one in October 2007 (5 h and 35 mCrab). During both outbursts the average 20–60 keV X-ray spectrum was well fit by a power law ($\Gamma \sim 2.5$) or, alternatively, by a bremsstrahlung model ($kT \sim 40$ keV). In addition, a possible cyclotron resonance feature around 25 keV was reported by Grebenev & Sunyaev (2010), although the authors could not draw any conclusion on the genuine existence of such a feature. As for the soft X-ray band (0.5–10 keV), IGR J18462–0223 was observed by *XMM-Newton* for 32 ks on April 2011 (Bodaghee et al. 2012). Its X-ray spectrum is modeled well by an absorbed power law that yields a high

Table 1. Summary of the characteristics of all hard X-ray outbursts detected by INTEGRAL/IBIS from IGR J18462–0223 to date.

<i>N.</i>	Peak-date (MJD)	Energy band (keV)	Duration (h)	Significance (σ)	Peak-flux ($\text{erg cm}^{-2} \text{s}^{-1}$)	Average flux ($\text{erg cm}^{-2} \text{s}^{-1}$)	Γ (power law)
1* [‡]	~53853.40	18–60	~1	7.8	$(1.5 \pm 0.2) \times 10^{-9}$	4.0×10^{-10}	$2.2^{+0.7}_{-0.7}$
2	~53981.20	18–60	~12	8.2	$(2.6 \pm 0.7) \times 10^{-10}$	9.7×10^{-11}	$2.0^{+0.7}_{-0.7}$
3 (*)	~54385.75	18–60	~5	11.1	$(6.4 \pm 1.4) \times 10^{-10}$	2.6×10^{-10}	$2.4^{+0.6}_{-0.6}$
4	~54519.89	18–60	~1	5.7	$(7.0 \pm 1.7) \times 10^{-10}$	2.7×10^{-10}	
5	~54909.08	18–60	~4	5.7	$(7.0 \pm 2.1) \times 10^{-10}$	1.1×10^{-10}	

Notes. The table lists the date of their peak emission, energy band of the detection, approximate duration, and significance detection of the entire flaring activity, X-ray flux at the peak, average flux, and photon index of the power law spectrum. Outbursts number 2, 4, 5 are newly discovered while outbursts number 1 and 3, indicated by the symbol (*), have been already reported in the literature by Grebenev & Sunyaev (2010). ^(‡) Outburst also detected by INTEGRAL/JEM–X.

absorbing column density ($N_{\text{H}} \sim 3 \times 10^{23} \text{ cm}^{-2}$) and a photon index equal to $\Gamma \sim 1.5$. The unabsorbed X-ray flux is $3.6 \times 10^{-11} \text{ erg cm}^{-2} \text{ s}^{-1}$ (0.5–10 keV). An iron line at 6.4 keV and a break in the power law at 3 keV are also present in the X-ray spectrum. These spectral characteristics are typical of wind-fed accreting X-ray pulsars and, in fact, X-ray pulsations were also discovered at $\sim 997 \text{ s}$ (Bodaghee et al. 2012). The catalogued 2MASS infrared source nearest to the *XMM-Newton* error circle ($2''.5$ radius) is 2MASS J18461279–0222261/USNO B–1.0 0876–0579765, which is about $3''.4$ away, i.e. outside of it (Bodaghee et al. 2012).

Here we report on both soft (0.5–10 keV) and hard (18–60 keV) X-ray properties of IGR J18462–0223 during the out-of-outburst state, as obtained from archival *ASCA*, *Chandra*, *Swift*/XRT, and INTEGRAL/IBIS observations. We also report on INTEGRAL/IBIS and INTEGRAL/JEM–X spectral and timing analysis of three newly discovered fast X-ray outbursts. Next, we investigated the IBIS/ISGRI and RXTE/ASM long-term monitoring light curves of the source searching for orbital periodicities. Moreover, to explore the field of IGR J18462–0223 and investigate its longerwavelength counterpart, we acquired optical spectra of 2MASS J18461279–0222261 with the 3.58 m Telescopio Nazionale *Galileo* located on the Canary Islands (Spain) and deep *R*-band imaging of the source field with the 1.5 m *Cassini* telescope located in Loiano (Italy); we also retrieved near-infrared (NIR) images of the field collected within the UKIDSS Galactic Plane Survey (Lucas et al. 2008).

2. Data analysis

For the INTEGRAL study, we used all the public data collected with IBIS (Ubertini et al. 2003) from February 2003 to May 2011. In particular, the data set consists of 4742 pointings or Science Windows (ScWs, $\sim 2000 \text{ s}$ duration) where IGR J18462–0223 was within 12° from the centre of the instruments field of view (FoV), for a total on-source time of 6.96 Ms. A 12° limit was applied because the off-axis response of IBIS (whose FoV is $30^\circ \times 30^\circ$) is not well modeled at large angles and consequently may introduce a systematic error in the measurement of source fluxes. The data reduction was carried out with the release 9.0 of the Offline Scientific Analysis software (OSA). IBIS/ISGRI (Lebrun et al. 2003) images for each pointing were generated in the energy band 18–60 keV.

We also used unpublished soft X-ray observations of IGR J18462–0223 (0.5–10 keV) from the *ASCA*, *Chandra* and *Swift*/XRT archive. Throughout the paper, all spectral analysis

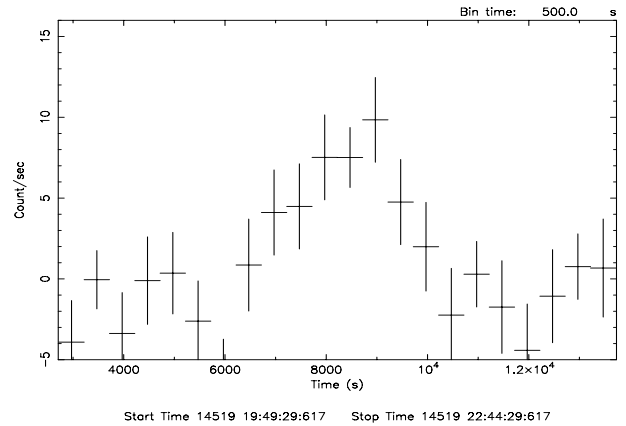


Fig. 1. IBIS/ISGRI light curve (18–60 keV) of a newly discovered fast X-ray outburst from IGR J18462–0223 (N. 4 in Table 1). The bin time is 500 s.

used *Xspec* version 11.3, and uncertainties are given at the 90% confidence level for one single parameter of interest.

3. INTEGRAL results

3.1. IBIS/ISGRI

3.1.1. Outbursts

An analysis at the ScW level of all the deconvolved IBIS/ISGRI shadowgrams (18–60 keV) was performed to search for new fast X-ray flares from IGR J18462–0223 detected with a significance greater than at least 5σ and lasting from a few hours to a few days. As a result, we report three newly discovered fast X-ray outbursts, which are listed in Table 1, together with the date of the peak emission, approximate duration, outburst detection significance, flux at outburst peak, average flux, and photon index of the power law spectrum. Since it was not possible to perform a meaningful spectral analysis for the outbursts having the lowest significance detection (N. 4 and 5 in Table 1), we assumed a Crab-like energy spectrum (photon index equal to 2.1) to calculate their fluxes.

The strongest, as well as shortest, newly discovered outburst (N. 4) was detected at 5.7σ level during only one ScW, lasting $\sim 1 \text{ h}$, at an off-axis angle of about 6.6 degrees. Figure 1 shows the IBIS/ISGRI light curve of the entire outburst activity with a bin time of 500 s. It reached a peak flux of $54 \pm 13 \text{ mCrab}$ or $(7.0 \pm 1.7) \times 10^{-10} \text{ erg cm}^{-2} \text{ s}^{-1}$ (18–60 keV) on 4 March 2008, its average flux during the entire outburst duration is equal to

2.7×10^{-10} erg cm⁻² s⁻¹. The limited statistics (5.7σ detection) prevent us from a meaningful spectral analysis. Another newly discovered fast X-ray outburst (N. 2) reached a 18–60 keV peak flux of 20 ± 6 mCrab or $(2.6 \pm 0.7) \times 10^{-10}$ erg cm⁻² s⁻¹ on 3 September 2003. The total outburst duration was ~ 12 h for a detection of 8.2σ . Its 18–60 keV spectrum is well fitted by a simple power law model with $\Gamma = 2.0_{-0.7}^{+0.7}$ ($\chi^2_\nu = 0.96$, 15 d.o.f.), the average flux (18–60 keV) is equal to 9.7×10^{-11} erg cm⁻² s⁻¹. Finally, the last newly discovered fast X-ray outburst (N. 5) was detected on 19 March 2009 at 5.7σ level with a duration of ~ 4 h. It reached a 18–60 keV peak flux of 54 ± 16 mCrab or $(7.0 \pm 2.1) \times 10^{-10}$ erg cm⁻² s⁻¹ while the average flux during the entire outburst is equal to 1.1×10^{-10} erg cm⁻² s⁻¹. As in the case of outburst N. 4, the limited statistics prevent us from a meaningful spectral analysis.

Table 1 provides a summary of the characteristics of all hard X-ray outbursts detected by INTEGRAL/IBIS from IGR J18462–0223 to date. We note that the newly discovered X-ray outbursts (N. 2, 4, 5) are similar, in terms of duration and spectral shape, to those previously reported in the literature (N. 1, 3) by Grebenev & Sunyaev (2010).

Grebenev & Sunyaev (2010) suggests there is a possible cyclotron resonance feature at ~ 26 keV in the summed X-ray spectra (20–60 keV) of two already published outbursts (N. 1 and 3 in Table 1). Bearing in mind that the X-ray outbursts N. 1, 2 and 3 in Table 1 have a very similar spectral shape within the large uncertainties, we summed them up with the aim of improving the statistics and investigating a possible cyclotron absorbing feature. A power law ($\Gamma = 2.1 \pm 0.5$, $\chi^2_\nu = 1.3$, 15 d.o.f.) provided a reasonable description of the average spectrum 18–60 keV. We therefore added a cyclotron absorption line (cyclabs in XSPEC notation) to the power law model, however no such feature was statistically required by the data. Further studies with much better statistics are needed to fully confirm whether such a feature truly exists.

3.1.2. Out-of-outburst emission

The out-of-outburst hard X-ray behavior of IGR J18462–0223 (18–60 keV) is totally unknown. We searched the entire IBIS/ISGRI public data archive for pointings where IGR J18462–0223 was within the fully coded FoV of IBIS ($9^\circ \times 9^\circ$). Subsequently we excluded those individual ScWs during which the source was in outburst. We collected a total of 371 ScWs to use to generate a mosaic significance map in the 18–60 keV band for a total exposure of 712 ks. IGR J18462–0223 was not detected, and we inferred a 18–60 keV 3σ upper limit of 0.6 mCrab or 8×10^{-12} erg cm⁻² s⁻¹ (again by assuming a Crab-like energy spectrum with photon index equal to 2.1). If we assume that the highest source flux takes place in an outburst during its peak (1.5×10^{-9} erg cm⁻² s⁻¹), as measured by IBIS/ISGRI in the energy range 18–60 keV, we can derive a dynamic range of >190 .

3.2. JEM–X

The X-ray Monitor JEM–X (Lund et al. 2003) onboard the INTEGRAL satellite observes simultaneously with IBIS/ISGRI, providing images in the energy band 3–35 keV with a $13^\circ 2$ diameter partially coded FoV (PCFoV). Images from JEM–X (3–20 keV) were created for all outbursts reported in Table 1. Because of the much smaller JEM–X PCFoV compared to the IBIS one ($30^\circ \times 30^\circ$), the source was inside the JEM–X PCFoV only in one case so that it was possible to extract a spectrum and

a X-ray light curve. In fact, during the outburst that occurred in April 2006 (N. 1 in Table 1) with ~ 1 h duration, the source was also detected by JEM–X at the 5.2σ level (3–20 keV) with an effective exposure time of ~ 1.7 ks. From the JEM–X light curve of the X-ray outburst binned with 100 seconds, we estimated a 3–10 keV (3–20 keV) source peak flux equal to 4.0 ± 0.7 (6.1 ± 1.1) $\times 10^{-10}$ erg cm⁻² s⁻¹. We extracted a JEM–X spectrum (3–20 keV) that was reasonably fitted with a simple power law model ($\chi^2_\nu = 0.96$, 131 d.o.f.) having a hard photon index ($\Gamma = 0.98 \pm 0.55$). Unfortunately, the JEM–X data only extend down to 3 keV, i.e. not low enough in energy to allow an investigation of the X-ray absorption. The average flux during the X-ray outburst was $\sim 1.0 \times 10^{-10}$ erg cm⁻² s⁻¹ (3–10 keV) and 2.2×10^{-10} erg cm⁻² s⁻¹ (3–20 keV). We also performed the broadband spectral analysis of the simultaneous JEM–X/ISGRI outburst spectrum: a good fit was achieved by a power law ($\chi^2_\nu = 1.09$, 139 d.o.f.) having $\Gamma = 1.3 \pm 0.5$ and a cross-calibration constant of $1.0_{-0.6}^{+1.7}$. The 3–60 keV average flux is equal to 5.7×10^{-10} erg cm⁻² s⁻¹.

4. Archival soft X-ray observations

4.1. ASCA

From archival ASCA data, we found that on April 1997 IGR J18462–0223 was inside the GIS2 FoV for ~ 22 ks during an observation of the ASCA Galactic plane survey (Sugizaki et al. 2001). We reduced the data and found that the source was not detected. A background count rate of 9.6^{-4} cts s⁻¹ was derived and then used it with WEBPIMMS in order to estimate a 0.5–10 keV 3σ upper limit of 2.9×10^{-13} erg cm⁻² s⁻¹. We assumed the same spectral model of the *Swift*/XRT observation. If we consider that the highest source flux takes place in an outburst as detected by INTEGRAL/JEM–X in a similar energy range, then we can infer a dynamic range of >1380 .

4.2. *Swift*/XRT

A search in the *Swift* (Gehrels et al. 2004) X-ray telescope (XRT, 0.2–10 keV, Burrows et al. 2005) data archive revealed that XRT was pointed at IGR J18462–0223 (source on-axis) on 12 November 2011 for a total exposure of ~ 2 ks.

XRT data reduction was performed using the XRTDAS standard data pipeline package (XRTPIPELINE v. 0.12.6), in order to produce screened event files. All data were extracted only in the Photon Counting (PC) mode (Hill et al. 2004), adopting the standard grade filtering (0–12 for PC) according to the XRT nomenclature. Events for spectral analysis were extracted within a circular region of radius $20''$, centered on the source position, which encloses about 90% of the PSF at 1.5 keV (see Moretti et al. 2004). The background was taken from various source-free regions close to the X-ray source of interest, using circular regions with different radii to ensure an evenly sampled background. In all cases, the spectra were extracted from the corresponding event files using the XSELECT software. We used v. 013 of the response matrices and created individual ancillary response files *arf* using XRTMKARF v. 0.6.0. IGR J18462–0223 was detected at $\sim 13\sigma$ level, and the best determined XRT position is at RA = $18^{\text{h}}46^{\text{m}}12.84^{\text{s}}$, Dec = $-02^\circ 22' 29''.7$ (J2000) with the error radius being equal to $2''.4$ ¹. Such coordinates are $2''.4$

¹ 90% c.l., we used the XRT–UVOT alignment and matching UVOT field sources to the USNO-B1 catalog, see Evans et al. (2009) and http://www.swift.ac.uk/user_objects

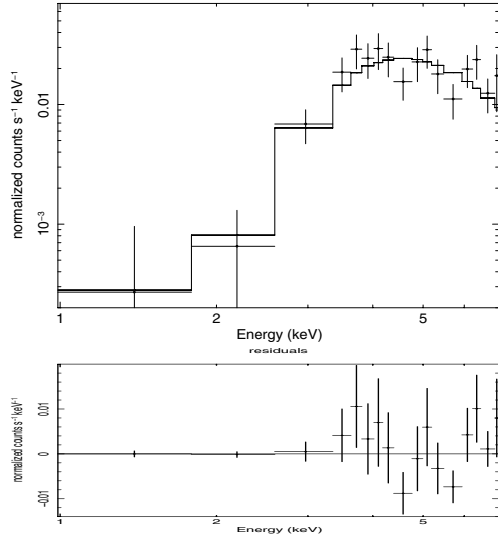


Fig. 2. *Swift*/XRT spectrum of IGR J18462–0223 best fitted by an absorbed power law model (*top*) and relative residuals (*bottom*).

from (and compatible with) the *XMM-Newton* position reported by Bodaghee et al. (2012) with an error radius of $2''.5$ (see Fig. 7 and relative discussion in Sect. 6).

From the *Swift*/XRT data, it was possible to extract a meaningful spectrum only in the energy range 1–7 keV. Below 1 keV and above 7 keV, the statistics are not good enough to perform a reliable spectral analysis. Because of the small number of counts, we used the Cash statistic on the unbinned data (Cash 1979). First the spectrum was fitted by an absorbed power law where the absorption was fixed to the Galactic value of $1.85 \times 10^{22} \text{ cm}^{-2}$ (Kalberla et al. 2005); however, the fit (C-statistics/d.o.f. = 496/598) was characterized by a hard photon index, and the residuals strongly suggested that there was extra absorption at lower energies. The addition of an intrinsic absorption significantly improved the fit (C-statistics/d.o.f. = 380/597; $\Delta C = 116^2$). The best fit parameters are $\Gamma = 1.7^{+0.2}_{-0.2}$ and intrinsic $N_{\text{H}} = (19.7^{+5.7}_{-4.6}) \times 10^{22} \text{ cm}^{-2}$ (see spectrum in Fig. 2), which are values that are fully compatible within the uncertainties with those obtained with *XMM-Newton* (Bodaghee et al. 2012). In particular, the intrinsic N_{H} measured by both *XMM-Newton* and *Swift*/XRT (i.e. $\sim 3 \times 10^{23} \text{ cm}^{-2}$) is higher than that characterizing other classical SFXTs (i.e. $\sim 10^{22} \text{ cm}^{-2}$). The *Swift*/XRT 0.5–10 keV absorbed (unabsorbed) average flux is $1.6 \times 10^{-11} \text{ erg cm}^{-2} \text{ s}^{-1}$ ($2.7 \times 10^{-11} \text{ erg cm}^{-2} \text{ s}^{-1}$). We note that this is a flux state similar to the one measured by *XMM-Newton* (unabsorbed $3.6 \times 10^{-11} \text{ erg cm}^{-2} \text{ s}^{-1}$) in the same energy band. A light curve was extracted from the *Swift*/XRT data and we noted that the source flux remained constant, within errors, with no sign of flaring activity throughout the duration of the observation.

4.3. *Chandra*

The ACIS-I detector onboard *Chandra* observed IGR J18462–0223 on 27 October 2008 for a total exposure time of ~ 1 ks. We reduced the data using the latest *Ciao* software (v 4.4) and calibration file. No source was detected inside the ACIS-I FoV, and we derived a background count rate of 0.05 cts s^{-1} and

² On the basis of the Wilks theorem (1938, 1963), Cash demonstrates that ΔC is distributed as $\Delta\chi^2$, and consequently the confidence levels are determined in the same way as for the χ^2 statistics.

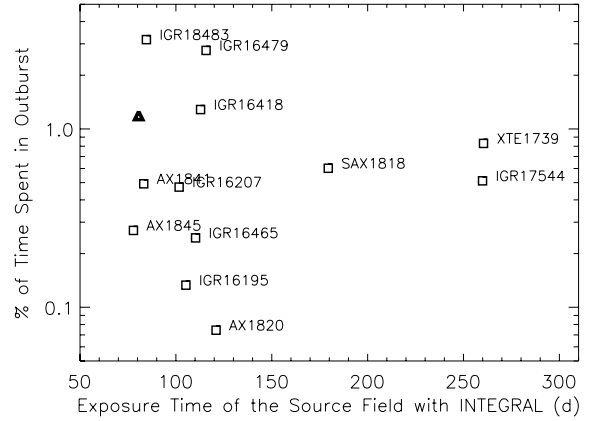


Fig. 3. Percentage of time spent in outburst vs exposure time (days) for a sample of 13 firm/candidate SFXTs as taken from Ducci et al. (2010). IGR J18462–0223 is indicated by means of a black triangle.

then used it with WEBPIMMS in order to estimate a 0.5–10 keV 3σ upper limit of $7.1 \times 10^{-12} \text{ erg cm}^{-2} \text{ s}^{-1}$. We assumed the same spectral model of the *Swift*/XRT observation.

5. Recurrence time of the outbursts and duty cycle

5.1. *INTEGRAL*

The sky region of IGR J18462–0223 has been covered by *INTEGRAL*/IBIS observations for a total exposure time of ~ 7 Ms. *INTEGRAL*/IBIS monitoring could be considered as a sporadic sampling of the light curve with a resolution of 2000 s over a baseline of about eight years. We calculated the duty cycle of IGR J18462–0223 (i.e. the fraction of time spent in bright outbursts with respect to the total observational time) following the same criteria as adopted by Ducci et al. (2010); i.e., we considered the duration of only the bright outbursts detected with a significance level greater than at least 5σ . As a result the duty cycle is $\sim 1.2\%$. In Fig. 3 we compare it with those of a sample of firm/candidate SFXTs analyzed by Ducci et al. (2010). We note that it is in the range 0.1%–3% found by Ducci et al. (2010).

It is intriguing to note that all the outbursts detected by *INTEGRAL* to date (see Table 1) are spaced by multiples of ~ 2 days. In fact if we assume the occurrence time of the n th outburst as given by $T_n = T_0 + (nT_{\text{orb}})$, where $T_0 = 53853.4$ MJD is the time of the first ever detected outburst, then we found that $T_{\text{orb}} = 2.13$ days is the longest time able to account for the peak occurrence of all the detected outbursts. In fact, the times predicted by the $T_{\text{orb}} = 2.13$ days periodicity (53981.20 at cycle $n = 60$, 54385.90 at $n = 250$, 54520.09 at $n = 313$, 54909.88 at $n = 496$) are in very good agreement with those observed by *INTEGRAL* at the peak (see Table 1) if we consider the outbursts duration to be on the order of hours. This hint of a possible 2.13 days periodicity could be interpreted as the likely orbital period of the binary system. As the next step, to search for any evidence of periodicity by using a proper analysis, we investigated the IBIS/ISGRI long-term light curve with the Lomb-Scargle periodogram method by means of the fast implementation of Press & Rybicki (1989) and Scargle (1982). No signal having a significance level greater than at least 90% is seen in the periodogram at any period, in particular at ~ 2.13 days.

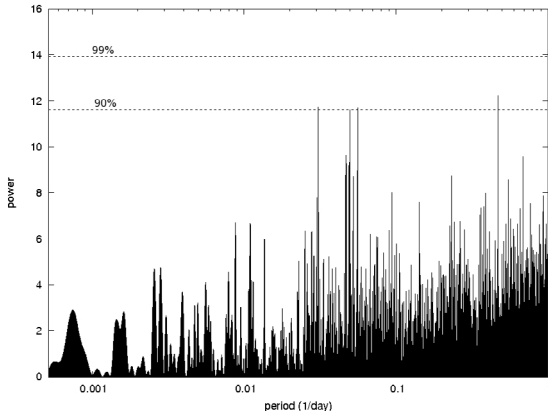


Fig. 4. Lomb-Scargle periodogram of IGR J18462–0223 RXTE/ASM dwell by dwell light curve. The two dotted lines represent the significance level of 90% and 99%, respectively. No significant signal is detected above 99%, the strongest peak is slightly above the 90% level and it corresponds to a period of 2.1378 days.

5.2. RXTE/ASM

The all-sky instrument ASM (Levine et al. 1996) onboard the RXTE satellite was an X-ray monitor consisting of three Scanning Shadow Cameras (SSCs), each with a position sensitive proportional counter. ASM measured the counts from IGR J18462–0223 with one of the three SSCs up to several times per day during ~ 90 s long dwells. From the ASM team web page³ we downloaded the long-term monitoring light curve (2–10 keV) covering the period from Jan. 1996 to Dec. 2009.

We investigated with Lomb–Scargle the long-term monitoring RXTE/ASM dwell-by-dwell light curve. The strongest peak is detected slightly above a significance level of 90% (see Fig. 4), and it corresponds to a period of ~ 2.1378 days, which agrees with the previously inferred value of 2.13 days. Other peaks are also present in the periodogram, although they do not exceed the 90% significance level. While this could appear unusual, we note that it is not the first time that a period has been detected in the light curve of one X-ray instrument and not in that of others (e.g. Drave et al. 2011; Clark et al. 2010). In fact, we note that the RXTE/ASM long-term monitoring light curve has a much longer baseline (14 years) than IBIS/ISGRI (8 years); in addition, ASM measure the source count rate up to several times per day, so the ASM light curve is well sampled throughout the 14 years, which is not the case for the IBIS/ISGRI light curve. This could possibly explain why a hint of periodicity has only been observed in the RXTE/ASM periodogram.

As a crosscheck, we also downloaded the fast Fourier transform power density spectrum of IGR J18462–0223 as obtained from the ASM team web page by using the standard criteria mentioned there (i.e., by averaging the light curves into 0.05 day bins, subtracting the mean value of all inhabited bins from each inhabited bin, and taking a fast Fourier transform, the resulting power in each frequency bin is divided by the average power over the whole frequency range). As seen from Fig. 5, the strongest peak in the periodogram again corresponds to a period of ~ 2.1377 days. Unfortunately we cannot claim a secure detection and draw any firm conclusion on the actual presence of a 2.13 day periodicity in the RXTE/ASM data because of the low statistical significance ($\sim 90\%$) of the tentative detected periodicity.

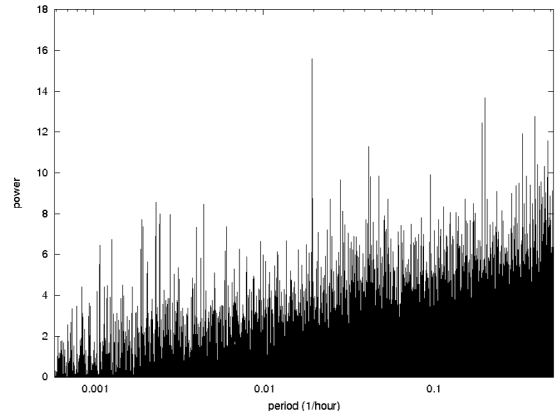


Fig. 5. Fast Fourier transform periodogram of IGR J18462–0223 RXTE/ASM dwell by dwell light curve as downloaded from the ASM team web page⁴ and obtained by using the standard criteria mentioned there. The strongest peak corresponds to a period of 2.1377 days.

6. Search for the optical/near-infrared counterpart

To explore the field of IGR J18462–0223 and investigate its proposed counterpart, we followed several approaches. First, in order to conclusively exclude as the optical counterpart the nearest cataloged IR source 2MASS J18461279–0222261 mentioned by Bodaghee et al. (2012), starting at 02:49 UT on 2012 May 31 we acquired two 20-min optical spectra of it with the 3.58 m Telescopio Nazionale *Galileo*, located in the Canary Islands (Spain) and equipped with the DoLoRes instrument plus LR-B grism and a slit of width $1''.5$. These spectra were reduced following a standard procedure (Horne 1986) within IRAF⁵. As expected, given the position of 2MASS J18461279–0222261 with respect to the *XMM-Newton* and *Swift* positions of IGR J18462–0223 (see also Fig. 6), its optical spectrum does not show any peculiar feature and appears typical of a very reddened G-type star.

Next, we performed deep optical imaging on the *XMM-Newton* and *Swift*/XRT error circles to look for the presence of fainter objects within them. To this purpose we acquired two 20-min *R*-band exposures of the IGR J18462–0223 field with the 1.5 m “*Cassini*” telescope located in Loiano (Italy). The telescope carries the BFOSC instrument, with an EEV CCD that allows the coverage of a $13' \times 12.6'$ field on a scale of $0''.58/\text{pixel}$. Observations were performed starting at 21:29 UT of 2012 July 27, under an average seeing of $1''.9$.

The scientific frames were corrected for bias and flat field and then stacked together to increase their signal-to-noise ratio, again following a standard procedure. To get an estimate of the image depth, we performed a photometric study of it. Owing to the field crowdedness (see Fig. 6), we chose standard point spread function (PSF) fitting technique by using the PSF-fitting algorithm of the DAOPHOT II image data-analysis package (Stetson 1987) running within MIDAS⁶.

⁴ http://xte.mit.edu/ASM_lc.html

⁵ IRAF is the Image Analysis and Reduction Facility made available to the astronomical community by the National Optical Astronomy Observatories, which are operated by AURA, Inc., under contract with the US National Science Foundation. It is available at <http://iraf.noao.edu/>

⁶ MIDAS (Munich Image Data Analysis System) is developed, distributed and maintained by the European Southern Observatory and is available at <http://www.eso.org/sci/software/esomidas/>

³ http://xte.mit.edu/ASM_lc.html

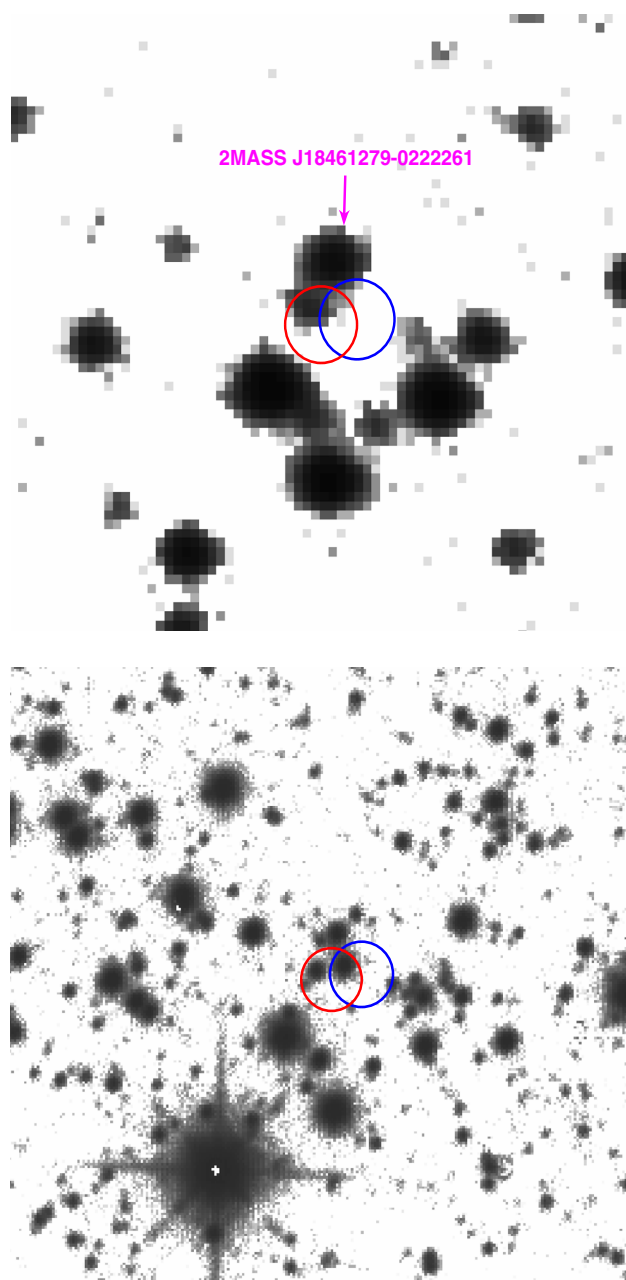


Fig. 6. *R*-band image acquired with the “Cassini” telescope plus BFOSC (*upper panel*) and UKIDSS *K*-band image (*lower panel*) of the field of IGR J18462–0223, both with the 90% confidence level *XMM-Newton* and *Swift* X-ray error circles (the right (blue) and the left (red) one, respectively superimposed). For both images, the field size is about $40'' \times 40''$; north is at the top and east to the left. The 2MASS object mentioned by Bodaghee et al. (2012) is also labeled and indicated with an arrow in the *upper panel*, whereas the counterpart we propose in this paper is the NIR object in the *lower panel* contained within the intersection of the *Swift* and the *XMM-Newton* error circles.

The image thus acquired was then also processed with the GAIA/Starlink⁷ package to obtain an astrometric solution based on 30 USNO-A2.0⁸ reference stars in the field of

⁷ Available at <http://star-www.dur.ac.uk/~pdraper/gaia/gaia.html>

⁸ The USNO-A2.0 catalog is available at <http://archive.eso.org/skycat/servers/usnoa>

IGR J18462–0223. The conservative error in the optical position is $0''.58$, which was added in quadrature to the systematic error in the USNO catalog ($0''.25$ according to Assafin et al. 2001; and Deutsch 1999).

The final 1σ uncertainty in the astrometric solution of the image is thus $0''.63$. Once we had determined the astrometry of the image, we superimposed it with the *XMM-Newton* and *Swift* X-ray error circles. The result is reported in the upper panel of Fig. 6; no objects are present within the *XMM-Newton* error circle down to a $3\text{-}\sigma$ magnitude limit⁹ of $R < 21.5$, while an object lying southeast of 2MASS J18461279-0222261 and of magnitude $R = 18.76 \pm 0.04$ is contained in the *Swift* positional uncertainty. This source has coordinates (J2000) RA = $18^{\text{h}}46^{\text{m}}12^{\text{s}}.90$, Dec = $-02^{\circ}22'28''.8$.

Finally, to better explore this source and the NIR content of the two X-ray error circles we searched the UKIDSS Galactic Plane Survey (Lucas et al. 2008) for NIR images of the field (see Fig. 6, lower panel). We found *JHK* frames acquired on 12 June 2006 and clearly detect the above object at magnitudes $J = 15.397 \pm 0.005$, $H = 14.760 \pm 0.004$ and $K = 14.341 \pm 0.009$. These values and the associated colors are actually not typical of a reddened blue giant counterpart of an SFXT, which is expected to be much brighter in the NIR. We thus consider this source as also an unlikely counterpart for IGR J18462–0223.

In the UKIDSS images we moreover detected a number of other objects within or close to the *Swift* and the *XMM-Newton* X-ray error circles (as can be seen in the lower panel of Fig. 6); however, a more careful look shows just one single NIR object within their intersection: this source appears rather bright in the *K*-band image and is undetected in the *J*-band one. Its UKIDSS coordinates (J2000) are RA = $18^{\text{h}}46^{\text{m}}12^{\text{s}}.757$, Dec = $-02^{\circ}22'28''.48$ (the uncertainty is about $0''.1$; Lucas et al. 2008), and the NIR magnitudes are $J > 19.5$, $H = 15.714 \pm 0.010$ and $K = 13.178 \pm 0.003$ (for the *J*-band we used the survey limit as reported in Casali et al. 2007). We notice that the UKIDSS astrometry is fully consistent with the X-ray and the optical ones within the uncertainties, and that the photometry is as well consistent with the 2MASS one (Skrutskie et al. 2006) of isolated field stars. We also notice that this source is positionally coincident (within $0''.25$) with the mid-IR GLIMPSE catalog source G030.2231+00.0791 (Benjamin et al. 2003).

All of the above strongly indicates that this very source, which lies at the intersection of the two X-ray positional uncertainties, might be a very reddened blue supergiant and the actual counterpart of IGR J18462–0223. As a corollary, this finding indicates that the two X-ray positions are not in disagreement but instead allow the discovery of the NIR counterpart of this hard X-ray object by being considered together.

7. Summary and discussion

We presented a comprehensive multiwavelength study of the poorly known candidate SFXT IGR J18462–0223, at X-rays in the energy bands 0.5–10 keV and 18–60 keV and in both the outburst and out-of-outburst state, as well as in optical and NIR bands.

The joint soft X-ray positional information obtained with *Swift*/XRT and *XMM-Newton*, together with optical and

⁹ We stress that the *R*-band magnitude calibration was obtained using USNO-A2.0 stars in the field, which are known to have systematic uncertainties of up to a few tenths of magnitude in some cases (see Masetti et al. 2003), thus the magnitudes reported above may suffer from a systematic shift of this amount.

Table 2. Summary of characteristics of all soft X-ray observations targeted at IGR J18462–0223 to date.

Date (MJD)	Energy band (keV)	X-ray satellite	Exposure (ks)	Average flux (erg cm ⁻² s ⁻¹)	X-ray state	Γ (power law)	N _H (10 ²² , cm ⁻²)
50 561.00	0.5–10	ASCA	22	<2.9 × 10 ^{-13‡}	quiescence		
53 853.35	3–10	INTEGRAL/JEM-X	2	1.0 × 10 ⁻¹⁰	outburst	0.98 ± 0.55	
54 766.65	0.5–10	<i>Chandra</i>	1	<7.1 × 10 ^{-12‡}	quiescence		
55 669.37*	0.5–10	XMM	32	3.6 × 10 ⁻¹¹	intermediate	1.5 ± 0.1	28 ± 1
55 877.80	0.5–10	<i>Swift</i> /XRT	2	2.7 × 10 ⁻¹¹	intermediate	1.7 ± 0.2	19.7 ^{+5.7} _{-4.6}

Notes. The table lists the date of the observation, energy band and X-ray satellite performing the observation, exposure time, unabsorbed average flux, X-ray state of the source, photon index and total absorption of the power law spectrum. (‡) 3σ upper limit. The observation indicated by the symbol (*) has been already reported in the literature by Bodaghee et al. (2012).

NIR observations, allowed us to pinpoint the very likely counterpart of this hard X-ray object as a very red source with characteristics that are fully consistent with those of a heavily reddened early-type supergiant. Assuming thus a blue supergiant nature for the secondary component of the X-ray binary IGR J18462–0223, we can determine the reddening toward the source by considering the intrinsic NIR colors of such stars (Wegner 1994). In the present case, we observe $H - K = 2.54$, whereas the intrinsic value of this color is $(H - K)_0 \sim 0$ for early-type supergiants, which implies a color excess of $E(H - K) \sim 2.5$. Using the Milky Way extinction law of Cardelli et al. (1989), this means a reddening $A_V \approx 40$ mag, or $A_K \approx 4$ mag. This is of course consistent with not detecting the object in the R band, and also in the J one given that a magnitude $J \sim 22.5$ is expected for the source in this scenario, thus well below the UKIDSS limit in this band.

This reddening, when using the formula of Predehl & Schmitt (1995), implies a column density $N_H \sim 6.4 \times 10^{22}$ cm², which is higher than that of the Galaxy along the line of sight of the source, but lower than measured in X-rays (see Table 2). This suggests that (i) the object is very far from Earth, possibly on the far side of the Galaxy; and (ii) additional extinction is present in the vicinity of the accretor. Concerning point (i) we can try to estimate the distance of IGR J18462–0223 again in the assumption that it hosts an OB supergiant. Using $A_V \sim 40$ mag and the tabulated absolute magnitudes (Lang 1992) and colors (Wegner 1994) for this type of star, we find a distance of ~ 11 kpc, thus consistent with a Scutum arm tangent location for the source as suggested by Bodaghee et al. (2012).

For the X-ray emission, and in particular the X-ray outburst behavior, if we assume a distance of ~ 11 kpc then IGR J18462–0223 displays peak-outburst X-ray luminosities in the range $\sim (4-22) \times 10^{36}$ erg s⁻¹ (18–60 keV) or 5.8×10^{36} erg s⁻¹ (3–10 keV), i.e. values similar to those of known confirmed SFXTs. Remarkably, the duration of all the X-ray outbursts detected by INTEGRAL is a few hours, i.e. in the range 1–12 h. Grebenev & Sunyaev (2010) argues that this characteristic could be an observational effect related to the source’s large distance or, alternatively, to its location at the edge of the INTEGRAL/IBIS FoV when detected during the outbursts, i.e. a region where the effective area of the telescope decreases. We tend to favor the former hypothesis since some outbursts have been detected by INTEGRAL/IBIS at a low off-axis angle (e.g. $\sim 6^\circ$). It is likely that, due to the relatively large distance of the source (~ 11 kpc), only the brightest ($L_X \geq 10^{36}$ erg s⁻¹) and shortest (few hours duration) tops of the outbursts are detectable, while the longer and lower intensity X-ray outburst activity is just too faint to be detected at energies above 18 keV. We found that the time IGR J18462–0223 spends in bright outbursts (as

detected by INTEGRAL) is $\sim 1.2\%$ of the total. This value is in the range 0.1%–3% found by Ducci et al. (2010), who analyzed INTEGRAL data of a sample of firm/candidate SFXTs.

From archival INTEGRAL/IBIS observations, we placed a 3σ upper limit of $\sim 8 \times 10^{-12}$ erg cm⁻² s⁻¹ (1.1×10^{35} erg s⁻¹ at 11 kpc) on the hard X-ray emission during the out-of-outburst state (18–60 keV). This is the most stringent constrain above 18 keV to date. Archival ASCA and *Chandra* observations also allowed us to infer a deep 3σ upper limit on the soft X-ray flux (0.5–10 keV) of the order of 2.9×10^{-13} erg cm⁻² s⁻¹, which translates into a luminosity of $L_X < 4.1 \times 10^{33}$ erg s⁻¹ at 11 kpc. This value implies a lower limit on the dynamic range equal to >1380 (0.5–10 keV). It is very likely that ASCA and *Chandra* observed the source during its soft X-ray quiescence which is a very rare state for SFXTs, since it is characterized by no accretion, luminosity values of $L_X \sim 10^{32}$ erg s⁻¹ and a very soft X-ray spectrum (e.g. see int’Zand 2005). Conversely, we reported a *Swift*/XRT detection with an absorbed flux (luminosity) of 1.6×10^{-11} erg cm⁻² s⁻¹ (2.3×10^{35} erg s⁻¹ at 11 kpc). Such a value is at least two orders of magnitudes higher than those inferred from the ASCA and *Chandra* observations during the likely quiescence; moreover, it is about one to two orders of magnitude lower than those typically measured during X-ray outbursts. It is likely that our reported *Swift*/XRT detection of the source, in addition to the XMM one reported by Bodaghee et al. (2012) with a similar flux, represents the so-called intermediate intensity X-ray state during which SFXTs spend the majority of their time (Sidoli et al. 2008) with typical $L_X \sim 10^{34}$ erg s⁻¹ and hard X-ray spectra ($\Gamma \sim 1-2$). During this intermediate X-ray state, SFXTs are still accreting material although at a much lower level than during the bright X-ray outbursts (Sidoli et al. 2008). The hard X-ray spectrum ($\Gamma \sim 1.5$) and the X-ray flux values measured by both *Swift*/XRT and XMM are compatible with the intermediate intensity state scenario.

We found a hint of a possible periodicity of ~ 2.13 days since all five X-ray outbursts detected by INTEGRAL/IBIS to date are spaced by multiples of 2.13 days. This periodicity could be interpreted as the likely orbital period of the binary system. Unfortunately we cannot draw any firm conclusion on its genuine existence because no unambiguous and significant signal (e.g. significance $>99.99\%$) at 2.13 days has been found with an adequate periodicity analysis. In fact, we note that in both RXTE/ASM periodograms obtained with two different methods (Lomb–Scargle and fast Fourier transform), a 2.13 days periodicity has been detected with a significance that is too low ($\sim 90\%$) to claim a secure and firm detection.

We note that Bodaghee et al. (2012) have recently detected X-ray pulsations at ~ 997 s from IGR J18462–0223. If we suppose that the tentative orbital period of 2.13 days is real, then

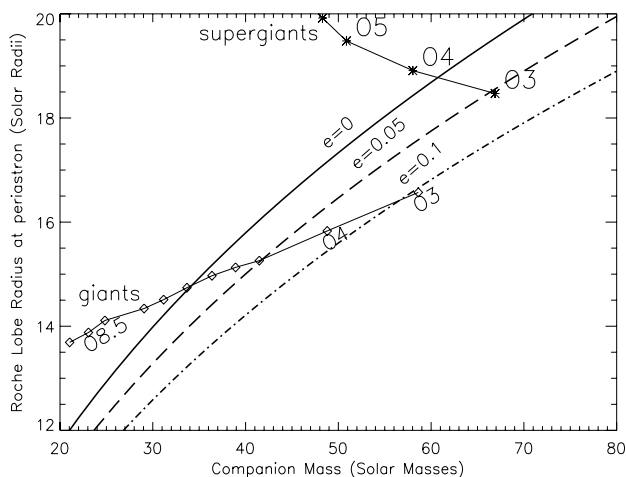


Fig. 7. Roche lobe radius at periastron versus the companion mass, assuming an orbital period of 2.13 days, for different eccentricities (solid line: $e=0$; dashed line: $e = 0.05$; dash-dotted line: $e = 0.1$). Radii and masses of O-type stars are also overplotted, taken from Martins et al. (2005): diamonds mark O-type giant stars (luminosity class III), while asterisks indicate O-type supergiants (luminosity class I), for different spectral subtypes.

this would nicely place the system in the region of the Corbet diagram, which hosts the wind-fed SGXBs and some other SFXTs (IGR J17544–2619, Drave et al. 2012; IGR J16418–4532, Sidoli et al. 2012); however, the same holds also for significantly longer orbital periods, i.e. up to ~ 30 – 40 days.

More importantly, if we suppose that the tentative orbital period of 2.13 days is real, then IGR J18462–0223 would be the SFXT with the shortest orbital period among the currently known systems. First, this scenario poses the question of whether a massive early-type OB supergiant star is compatible with such a short orbital period. Assuming that the compact object is a neutron star with a mass of $1.4 M_{\odot}$, we plot in Fig. 7 the Roche lobe radius of the companion (at periastron, if the orbit is not circular) versus its mass and for different system eccentricities (Eggleton 1983). The radii of O type stars, both I and III luminosity classes (Martins et al. 2005), are overplotted for comparison. From this plot it is evident that a typical O type supergiant, hence an SFXT nature, would be compatible with the 2.13 day orbital period. Also early type giant stars (earlier than O6, if the orbit is circular) represent viable possibilities as donor stars in IGR J18462–0223.

In addition, it is worth noting that in the scenario of IGR J18462–0223 with a short orbital period, its OB supergiant star would not necessarily fill its Roche lobe and other effects could also take place. In fact since the supergiant donor star expands and is close to fill its Roche lobe, the wind could not be spherically symmetrical (as for isolated stars), but instead strongly enhanced toward the compact object (focused wind), as e.g. in the case of the persistent SGXB Cyg X-1 (Friend & Castor 1982). Moreover, Sidoli et al. (2012) using a 40 ks *XMM-Newton* observation recently proposed that the neutron star hosted in the narrow orbit of the SFXT IGR J6418–4532 (~ 3.7 days orbital period) could be accreting in a regime that is transitional between pure wind and full Roche lobe overflow.

In such a scenario the mass loss from the supergiant star is dominated by the strong wind, but with the additional contribution of a tidal gas stream, focused toward the neutron star compact object. This mechanism produces extreme variations in the mass accretion rate (mainly due to the dynamical interaction

of the weak tidal gas stream with the accretion bow shock around the neutron star) and is responsible for the observed marked X-ray variability on a short timescale. Interestingly, Sidoli et al. (2012) propose that such a transitional Roche lobe overflow scenario could be a dominant process, not only in the case of the SFXT IGR J6418–4532, but also in other SFXTs with similar short orbital periods, such as our specific case of IGR J18462–0223. To date, the only available long (~ 30 ks), soft X-ray observation (*XMM*) of IGR J18462–0223 has recently been reported by Bodaghee et al. (2012); the source was detected at an intermediate flux level of $\sim 3 \times 10^{-11} \text{ erg cm}^{-2} \text{ s}^{-1}$ (0.5–10 keV) with a variability of an order of magnitude on timescales as short as ~ 15 min. Unfortunately, other soft X-ray observations are still lacking and are urgently needed to fully explore and consider whether a transitional Roche lobe overflow is occurring. Presently it is puzzling to explain how an SFXT with a short orbital period, like IGR J18462–0223, could spend a considerable fraction of time at very low X-ray luminosities out-of-outbursts, as inferred especially from INTEGRAL long-term monitoring above 18 keV ($L_X < 10^{35} \text{ erg s}^{-1}$). One possible explanation is that some mechanisms could likely be at work to reduce/stop the mass accretion rate onto the neutron star, i.e. centrifugal and/or magnetic barrier (Bozzo et al. 2008, Grebenev et al. 2007) or transitions between two different regimes of plasma cooling (Shakura et al. 2012).

Further studies of IGR J18462–0223, especially a long-term monitoring across all orbital phases, would be very useful to test the above models. Moreover, further investigations are urgently needed to fully confirm (or reject) the genuine existence of the putative 2.13 days periodicity. Also, NIR spectroscopy is needed to definitely confirm the nature of the reddened UKIDSS source presented in this paper as the likely counterpart to IGR J18462–0223 and its association with this interesting hard X-ray object.

Acknowledgements. We are very grateful to the referee, Ignacio Negueruela, for several important comments which substantially improved this paper. The Italian authors acknowledge the ASI financial support via grant ASI-INAF I/033/10/0 and I/009/10/0. This work was also supported by the grant from PRIN-INAF 2009 (The transient X-ray sky: new classes of X-ray binaries containing neutron stars, PI: Sidoli). S. P. Drave acknowledges support from the Science and Technology Facilities Council, STFC. This research made use of the public access RXTE/ASM light curves provided by the ASM team (see http://xte.mit.edu/ASM_lc.html). It has also made use of the VizieR catalog access tool at the CDS, Strasbourg, France. It was partly based on observations collected at the Italian Telescopio Nazionale *Galileo*, located at the Osservatorio del Roque de los Muchachos (Canary Islands, Spain) and at the “G.D. Cassini” telescope of the Astronomical Observatory of Bologna in Loiano (Italy). We thank Vania Lorenzi for coordinating our service mode observations at TNG, and Silvia Galletti and Antonio De Blasi for the acquisition of images in service mode at Loiano.

References

- Assafin, M., Andrei, A. H., Vieira Martins, R., et al. 2001, *ApJ*, 552, 380
- Benjamin, R. A., Churchwell, E., Babler, B. L., et al. 2003, *PASP*, 115, 953
- Bodaghee, A., Tomsick, J. A., & Rodriguez, J. 2012, *ApJ*, 753, 3
- Bozzo, E., Falanga, M., & Stella, L. 2008, *ApJ*, 683, 1031
- Cardelli, J. A., Clayton, G. C., & Mathis, J. S. 1989, *ApJ*, 345, 245
- Casali, M., Adamson, A., Alves de Oliveira, C., et al. 2007, *A&A*, 467, 777
- Cash, W. 1979, *ApJ*, 228, 939
- Clark, D. J., Sguera, V., Bird, A. J., et al. 2010, *MNRAS*, 406, L75
- Deutsch, E. W. 1999, *AJ*, 118, 1882
- Ducci, L., Sidoli, L., & Paizis, A. 2010, *MNRAS*, 408, 1540
- Drave, S. P., Clark, D. J., Bird, A. J., et al. 2011, *MNRAS*, 409, 1220
- Drave, S. P., Bird, A. J., Townsend, L. J., et al. 2012, *A&A*, 539, A21
- Eggleton 1983, *ApJ*, 268, 368
- Evans, P. A., Beardmore, A. P., Page, K. L., et al. 2009, *MNRAS*, 397, 1177
- Fiocchi, M., Sguera, V., Bazzano, A., et al. 2010, *ApJ*, 725, L68
- Friend, D. B., Castor, J. I. 1982, *ApJ*, 261, 293

- Gehrels, N., Chincarini, G., Giommi, P., et al. 2004, *ApJ*, 611, 1005
- Grebenev, S. A. 2010, Proc. of the Workshop, The Extreme sky: Sampling the Universe above 10 keV, PoS, 2009, 96, 60
- Grebenev, S. A., & Sunyaev, R. A. 2007, *A&A*, 33, L149
- Grebenev, S. A., & Sunyaev, R. A. 2010, *AstL*, 36, 533
- Hill, J. E., Burrows, D. N., Nousek, J. A., et al. 2004, Proc. SPIE, 5165, 217
- Horne, K. 1986, *PASP*, 98, 609
- in't Zand 2005, *A&A*, 441, L1
- Kalberla, P. M. W., Burton, W. B., Hartmann, D., et al. 2005, *A&A*, 440, 775
- Lang, K. R. 1992, *Astrophysical Data: Planets and Stars* (New York: Springer)
- Lebrun, F., Leray, J. P., Lavocat, P., et al. 2003, *A&A*, 411, L141
- Levine, A. M., Bradt, H., Cui, W., et al. 1996, *ApJ*, 469, 33
- Lucas, P. W., Hoare, M. G., Longmore, A., et al. 2008, *MNRAS*, 391, 136
- Lund, N., Budtz-Jorgensen, C., Westergaard, N. J., et al. 2003, *A&A*, 411, L231
- Martins, F., Schaerer, D., & Hillier, D. J. 2005, *AAP*, 436, 1049
- Masetti, N., Palazzi, E., Pian, E., et al. 2003, *A&A*, 404, 465
- Moretti, A., Campana, S., Tagliaferri, G., et al. 2004, Proc. SPIE, 5165, 232
- Negueruela, I., Smith, D., Reig, P., et al. 2006, *ESASP*, 604, 165
- Predehl, P., & Schmitt, J. H. M. M. 1995, *A&A*, 293, 889
- Press, W. H., & Rybicki, G. B. 1989, *ApJ*, 338, 277
- Scargle, J. D. 1982, *ApJ*, 263, 835
- Sguera, V., Barlow, E. J., Bird, A. J., et al. 2005, *A&A*, 444, 221
- Sguera, V., Bazzano, A., Bird, A. J., et al. 2006, *ApJ*, 646, 452
- Shakura, N., Postnov, K., Kochetkova, A., et al. 2012, *MNRAS*, 420, 216
- Skrutskie, M. F., Cutri, R. M., Stiening, R., et al. 2006, *AJ*, 131, 1163
- Sidoli, L., Romano, P., Mangano, V., et al. 2008, *ApJ*, 687, 1230
- Sidoli, L., Mereghetti, S., Sguera, V., et al. 2012, *MNRAS*, 420, 554
- Stetson, P. B. 1987, *PASP*, 99, 191
- Sugizaki, M., Mitsuda, K., Kaneda, H., et al. 2001, *ApJS*, 134, 77S
- Ubertini, P., Lebrun, F., Di Cocco, G., et al. 2003, *A&A*, 411, L131
- Wegner, W. 1994, *MNRAS*, 270, 229
- Wilks, S. S. 1938, *Ann. Mathematical Statistics*, 9, 60
- Wilks, S. S. 1963, *Mathematical Statistics* (Princeton University Press), Chap. 13
- Winkler, C., Courvoisier, T. J.-L., Di Cocco, G., et al. 2003, *A&A*, 411, L1
- Zurita Heras, J. A., & Chaty, S. 2008, *A&A*, 489, 657